Research Square

Preprints are preliminary reports that have not undergone peer review.
They should not be considered conclusive, used to inform clinical practice,
or referenced by the media as validated information.

Genome Wide Association Study of the Kynurenine Pathway

Chinh B'krong Nguyen
University of Bergen
Arve Ulvik
University of Bergen
Tore Ivar Aarsland
University of Bergen
Adrian McCann
Bevital (Norway)
Øyvind Helgeland
University of Bergen
Grete Seppola Tell
University of Bergen
Rolv T Lie
University of Bergen
Ottar Nygård
Haukeland University Hospital
Per Magne Ueland
Bevital (Norway)
Pål R Njølstad
University of Bergen
Jan Haavik
University of Bergen
stefan johansson
stefan.johansson@uib.no
University of Bergen

Article

Keywords: Tryptophan Catabolism, Pathway Regulation, GWAS, Immune-Metabolic Crosstalk

Posted Date: November 12th, 2026

DOI: https://doi.org/10.21203/rs.3.rs-10957011/v1

License: This work is licensed under a Creative Commons Attribution 4.0 International License.
Read Full License

Additional Declarations: Competing interest reported. Adrian McCann and Per Magne Ueland are employees at Bevital AS, a provider of targeted metabolomics services, which is owned by a non-profit foundation established to support research investigating vitamin B12 deficiency and related disorders.

Genome Wide Association Study of the Kynurenine Pathway

Chinh B'krong Nguyen[1], Arve Ulvik[2], Tore Ivar Aarsland[3], Adrian McCann[2], Øyvind Helgeland[1], Grethe Seppola Tell[4], Rolv T Lie[4], Ottar Nygård[6,7], Per Magne Ueland[2], Pål Rasmus Njølstad[1 8], Jan Haavik[3,5], Stefan Johansson[1,9]
1 Mohn Center for Diabetes Precision Medicine, Department of Clinical Science, University of Bergen, Norway
2 Bevital AS, Norway
3 Department of Biomedicine, University of Bergen, Norway
4 Department of Global Public Health and Primary Care, University of Bergen, Norway
5 Division of Psychiatry, Haukeland University Hospital, Bergen, Norway
6 Department of Heart Disease, Haukeland University Hospital, Bergen, Norway
7 Mohn Nutrition Research Laboratory, Department of Clinical Science, University of Bergen, 5020 Bergen, Norway
8 Department of Pediatric and Adolescent Medicine, Haukeland University Hospital, Bergen, Norway
9 Department for Medical Genetics, Haukeland University Hospital, Bergen, Norway
Corresponding authors: Chinh B'krong Nguyen & Stefan Johansson

Email: cng022@protonmail.com, stefan.johansson@uib.no
Author Contributions: CBN, AU, PMU, JH, ON, PRN, SJ designed the study. CBN quality-controlled and analyzed the data end-to-end. CBN and AU created graphical materials. CBN, AU, JH and SJ wrote the manuscript. GT and RL were involved in the recruitment of the cohort participants. All authors commented on the manuscript.

Conflict of interest: Adrian McCann and Per Magne Ueland are employees at Bevital AS, a provider of targeted metabolomics services, which is owned by a non-profit foundation established to support research investigating vitamin B12 deficiency and related disorders.

Classification: Biological Sciences, Metabolomics, Bioinformatics, Population Studies
Keywords: Tryptophan Catabolism, Pathway Regulation, GWAS, Immune-Metabolic Crosstalk

Abstract

The kynurenine pathway (KP) of tryptophan metabolism plays a key role in physiological processes such as neuronal modulation, aging and immunity. Although genome-wide association studies (GWAS) have identified genetic determinants of selected kynurenine metabolites, the genetic architecture of the pathway as a whole remains incompletely characterized.

We performed GWAS on nine KP metabolites and seven biologically informed metabolite-ratios measured by targeted liquid chromatography-tandem mass spectrometry (LC-MS/MS)

in 4,871 unrelated individuals of Norwegian ancestry from the Hordaland Health Study. We identified 23 independent metabolite-associated loci (mQTLs), including associations for all measured metabolites covering all enzymes in the initial part of the pathway. Many signals replicated known loci at key pathway genes, including IDO1/2, AFMID, KMO, KYNU, HAAO, AADAT while revealing how their effects propagate across multiple pathway intermediates and ratios.
Genetic associations were highly consistent with established pathway biology, with enzyme-specific loci predominantly affecting metabolites immediately upstream or downstream of the corresponding reaction. Ratio-based analyses identified additional hits not found by single-metabolite GWAS, reflecting pathway balance and vitamin B6-dependent enzymatic activity. Integration with expression quantitative trait locus data supported a dose-dependent role of KMO expression in regulating the kynurenic acid/quinolinic acid balance.
We also identified novel loci that may represent important amino acid metabolism-immune crosstalk in the regulation of KP and previously unrecognized links with fatty acid oxidation, phase II transformation and metabolite efflux processes.
Together, the study provides a comprehensive pathway-level view of the genetic determinants for circulating kynurenines and their ratios within a Northern European population.

Main Text

Introduction

The kynurenine pathway is the main catabolizing route for tryptophan (Trp) in both peripheral tissues and the central nervous system (CNS) (1). The pathway produces several intermediate metabolites (known as kynurenines) with immune and neuro-modulatory effects which have been related to numerous pathological conditions including cardiovascular diseases (2, 3), autoimmunity (4, 5), cancer(6, 7), preeclampsia(8), dementia and Parkinson's disease (9–11), Huntington's disease (12) and psychiatric disorders (13–15). Given its increasingly recognized importance in these conditions, this pathway has also been studied in model organisms including yeast, worms, flies and mice (16).

A schematic of the main steps of the kynurenine pathway is presented in Figure 1. The first step of the pathway is catalyzed by either the predominantly liver expressed tryptophan 2,3-dioxygenase (TDO2) or the ubiquitous indoleamine 2,3-dioxygenase (IDO1/2) (16) producing N-formyl kynurenine (fKyn) from tryptophan (Trp) which is rapidly converted to kynurenine (Kyn). Downstream reactions produce several bioactive intermediates including the side-branch metabolites kynurenic acid (KA), anthranilic acid (AA), xanthurenic acid (XA) and picolinic acid (Pic) and the core pathway 3-hydroxykynurenine (HK), 3-hydroxyanthranilic acid (HAA) and 2-amino-3-carboxymuconate semialdehyde (ACMS) *(Fig.1)*. Trp and several of the kynurenines, including Kyn, HK, and AA are able to cross the blood-brain barrier and are further converted to the neurotoxic QA, an agonist of the N-methyl-D-aspartate (NMDA) receptor or the neuroprotective KA, an antagonist of both the NMDA and α7 nicotinic acetylcholine receptors (15). In several tissues, QA is a substrate for further conversion to nicotinamide adenine nucleotide (NAD), a branch of the pathway known as *de novo* NAD+ synthesis. Two important cofactors of the pathway are pyridoxal 5'-phosphate (PLP), a B6 vitamer, and flavin adenine dinucleotide (FAD) *(Fig. 1).*

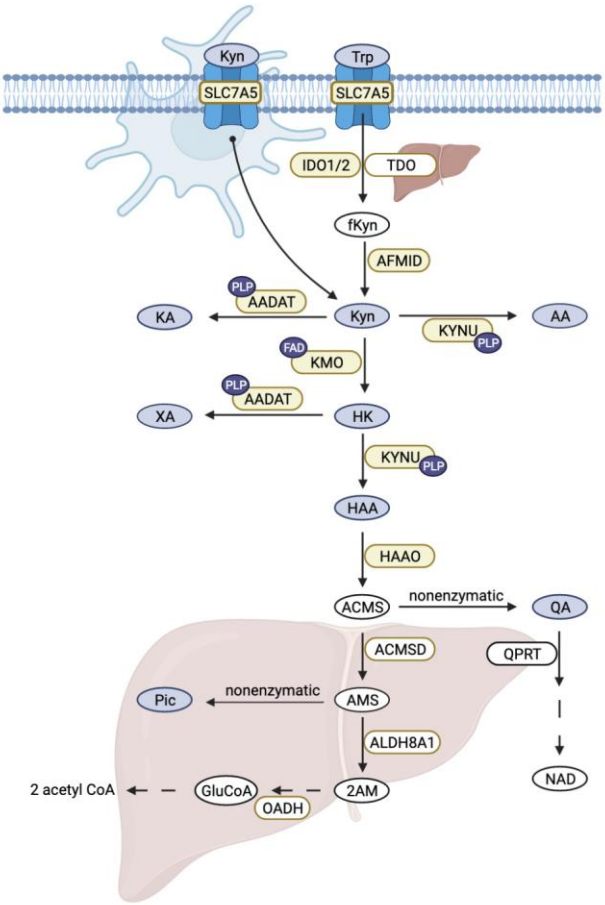


Fig 1.Tryptophan catabolism through the kynurenine pathway

The pathway is shown to complete with acetyl-coA as the final oxidized product. All studied metabolites are depicted as blue oval and known enzymes are depicted as rectangular blocks. Gene names are indicated, with those producing a hit in this study, in yellow background. Enzymes predominantly expressed in the liver are indicated. The first rate-limiting reaction that degrades tryptophan (Trp) is catalyzed either by tryptophan 2,3-dioxygenase (TDO2) or indoleamine 2,3-dioxygenase (IDO1/2). N-formylkynurenine (fKyn) is rapidly metabolized by arylformamidase (AFMID) to kynurenine (Kyn) which can subsequently branch into kynurenic acid (KA) by kynurenine/alpha-aminoadipate aminotransferase (AADAT), anthranilic acid (AA) by kynurenase (KYNU) and 3-hydroxykynurenine (HK) by kynurenine 3-monooxygenase (KMO). HK is converted further to either xanthurenic acid (XA) by AADAT or by KYNU to 3-hydroxyanthranilic acid (HAA).Next,3-hydroxyanthraniliate3,4-dioxygenase(HAAO)convertsHAAinto2-amino-3- carboxymuconate semialdehyde (ACMS) which either spontaneously cyclizes to quinolinic acid (QA) or is converted to 2-aminomuconate (AMS) by aminocarboxymuconate-semialdehyde decarboxylase (ACMSD). AMS can either spontaneously cyclize to picolinic acid (Pic) or be converted to glutaryl-coA (GlucoA) and further to acetyl-CoA. Other abbreviations: NAD nicotinamide; QPRT quinolinate phosphoribosyltransferase; ALDH8A1 aldehyde dehydrogenase 8 family member A1; OADH 2-oxo acid dehydrogenase. Two important co-factors of the pathway are vitamin B6/pyridoxal 5'phosphate (PLP) required for KYNU and AADAT and vitamin B2/flavin adenine dinucleotide (FAD) required for KMO. Figure generated by BioRender.

In many organisms, tryptophan metabolism is involved in nutrient sensing, mediating a balance between anabolic reactions and cellular stress defence and repair. In humans, tryptophan metabolism is involved in the maintenance and regulation of gut microbiota, autoimmune tolerance, tumor growth, acute inflammation, and regulation of mood and behaviour through production of neurotransmitters (21). Because of its involvement in so many vital processes there has been considerable interest in manipulating the kynurenine pathway, including developing inhibitors of key enzymes, in various clinical settings (21). For such strategies to succeed, detailed knowledge on pathway regulation is necessary. Genome wide association studies that use metabolite concentrations in blood or urine may provide insights into the regulation of the kynurenine pathway at the systemic level (23, 24). However, until recently, data has been obtained mostly on the most abundant metabolites (Trp and Kyn), and metabolites of particular interest like KA (24).

Although more data is accumulating, coverage of the kynurenine pathway remains incomplete and patchy. Metabolite ratios may provide more sensitive and specific indicators of enzyme or transporter activities than single metabolite concentrations. The ratio Kyn/Trp is widely accepted as a measure of IDO1-activation and has been linked to autoimmune diseases, cancer and inflammaging (6, 11, 19). Kyn/Trp is also positively associated with inflammatory markers such as neopterin (2), interferon-gamma (IFN-γ), interleukin (IL)-10 and tumor necrosis factor (TNF)-α(19). The ratio HK/(KA+XA+AA+HAA) [HKr], targets the two PLP-dependent enzymes kynurenine/α-aminoadipate aminotransferase (AADAT) and kynurenase (KYNU) and was recently suggested as a potential functional marker of vitamin B6 status (20). Two HKr sub-ratios, HK/(KA+XA) [HKr_a] and HK/(AA+HAA) [HKr_b], were also proposed to specifically capture AADAT and KYNU activity respectively (20). Other kynurenine-based ratios have been developed to reflect the status of the side branch vs. backbone reactions (pathway-balance) such as the KA/Kyn, Pic/QA and KA/QA ratios (9, 15). These ratios are of particular interest in neuropsychiatric conditions and the ratio KA/QA was recently dubbed the “neuroactive rheostat" (21).

Here we use data from 4,871 unrelated participants of a community-based cohort, the Hordaland Health Study (HUSK) (28) and performed Genome Wide Association studies (GWAS) on nine metabolites including Trp and eight kynurenines (Kyn, KA, AA, HK, HAA, XA, Pic, QA), measured by targeted LC-MS/MS as well as the ratios: Kyn/Trp, Kyn/KA, KA/QA, Pic/QA, HKr, HKr_a and HKr_b.

Results

Characteristics of the study population

6,757 genotyped samples were curated to obtain a sample of 4,931 unrelated individuals of Norwegian descent of which *N*=4,871 with available plasma metabolite measures were used for association analysis. The studied subjects represented two age groups of median age 48 years (53%) and 72 years (47%), whereof 56% were women. Other characteristics of the study cohort are presented in *Table S1A.*

GWAS of kynurenines

We performed GWAS for 16 traits **(**9 metabolites and 7 ratios) using 7,494,409 imputed variants with MAF>=1% and detected a total of 23 independent mQTLs/loci (indexed by 31

lead SNPs) with *P-value (P) < GWA level (5E-8)* associated with at least one metabolite or ratio *(Table 1 & Table S2)*. Among these 23 loci, 6 have not previously been linked to the kynurenine pathway. All studied traits, apart from Trp, showed at least one significant signal at the GWA level (*Fig. 2*). Manhattan plots and Quantile-Quantile (Q-Q) plots are illustrated in *Fig. S1.* Regional plots of each locus are displayed in *Fig. S2.* Summaries of previously reported GWA findings for molecular, metabolomic and clinical traits for the lead SNPs are given in *Tables S3-7* and *Table 2.*

Table 1: Significant trait-associated loci for all studied traits (8 metabolites and 7 ratios, no hits for Trp)

mQTL	Lead SNP	CHR:BP	Nearest gene	GWAS Result			Traits	Shared Traits[v]	References
				Beta	*P*	*EAF*			
1	***rs8050771***	16:87878570	*SLC7A5*	*0.024*	*1.92E-20*	*0,223*	***Kyn***, *Kyn/Trp*, *Kyn/KA*		Suhre-K et al 2011, Shin-S et al 2014, Long-T et al 2017, Lotta-L et al 2021, Surendran et al 2022
2	***rs6540080***	16:87818569	*KLHDC4 (SLC7A5)*	*-0.012*	*3.04E-08*	*0,334*	***Kyn***		Lotta-L et al 2021
3	***rs35441930[y]***	16:87828340	*SLC7A5*	*-0.012*	*3.10E-06*	*0,429*	***Kyn/Trp***		
4	***rs2160860***	8:39823145	*IDO1/2*	*-0.013*	*1.76E-09*	*0,366*	***Kyn,*** *QA*	*Kyn/Trp*	Shin-S et al 2014, Lotta-L et al 2021, Surendran et al 2022
5	***rs112281307***	17:76199376	*AFMID*	*0.069*	*1.09E-41*	*0,086*	***AA,*** *HKr_b*		Schlosser-P et al 2020
6	***rs111870199[y]***	17:76183773	*AFMID*	*0.050*	*3.27E-07*	*0,022*	***AA***		
7	***rs61825638***	1:241713402	*KMO*	*0.066*	*1.55E-58*	*0,265*	***KA/QA***, *KA, HKr_a, HKr, Kyn/KA, QA*	*HK, Pic/QA*	Long-T et al 2017, Lotta-L et al 2021, Surendran et al 2022
8	***rs6741488***	2:143793701	*KYNU*	*0.029*	*3.28E-19*	*0,266*	***AA***		Yin-X et al 2022, Surendran et al 2022
9	***rs75790387***	2:143634814	*KYNU*	*-0.098*	*8.82E-34*	*0,035*	***HKr_b***, *HKr, HK, HKr_a, AA*		Schlosser-P et al 2020
10	***rs34965832***	2:143750730	*KYNU*	*-0.050*	*9.99E-21*	*0,085*	***HKr_b***, *HKr, HK*		Yin-X et al 2022
11	***rs351684***	2:143721253	*KYNU*	*-0.026*	*5.64E-17*	*0,335*	***HKr_b***		
12	***rs17808482***	2:143750730	*KYNU*	*0.050*	*1.38E-09*	*0,036*	***HKr_b,*** *HKr*		Yin-X et al 2022
13	***rs55802110***	2:42997950	*HAAO*	*-0.033*	*7.61E-22*	*0,365*	***HAA,*** *HKr_b*		
14	***rs114679640***	2:43014172	*HAAO*	*0.081*	*1.40E-12*	*0,022*	***HAA***		
15	***rs112323196***	4:170960157	*AADAT*	*0.037*	*3.58E-13*	*0,087*	***KA***, *XA, KA/QA, Kyn/KA, HKr_a*		Surendran et al 2022
16	***rs887829***	2:234668570	*UGT1A4*	*0.039*	*4.35E-17*	*0,312*	***XA***		Yin-X et al 2022
17	***rs1408273***	6:25840946	*SLC17A3*	*-0.030*	*2.48E-12*	*0,467*	***XA***		Yin-X et al 2022, Surendran et al 2022
18	***rs1047891***	2:211540507	*CPS1*	*-0.024*	*3.13E-09*	*0,323*	***Pic***	*KA*	Yin-X et al 2022, Surendran et al 2022
19	***rs8056693***	16:20570661	*ACSM2B*	*0.091*	*3.51E-13*	*0,024*	***Pic,*** *Pic/QA*		Yin-X et al 2022
20	***rs57366670***	16:20578967	*ACSM2B*	*0.088*	*3.61E-09*	*0,017*	***Pic***		Yin-X et al 2022
21	***rs12920969***	16:89699523	*DPEP1*	*0.025*	*5.20E-11*	*0,469*	*Pic*	*Pic/QA*	Long-T et al 2017, Surendran et al 2022
22	***rs653178***	12:112007756	*ATXN2/SH2B3*	*0.017*	*5.95E-10*	*0,454*	***QA,*** *Kyn*	*KA/QA, Kyn/Trp*	Shin-S et al 2014
23	***rs4308309***	3:106034957	*CBLB*	*0.020*	*1.81E-08*	*0,466*	***KA/QA***		

*Hits were found using linear regression under the assumption of additive allelic effects of SNP dosages (minor allele) with lead SNP detected by stepwise-conditional regression on the top genome-wide hit of each 1Mb-clumped region; [Y] Discovered by conditional analysis. Each row corresponds to independent metabolite-quantitative locus (mQTL) illustrated by lead SNP, chromosomal/genomic position (CHR:BP), nearest gene and effect allele frequency (EAF)***. Numbering of mQTLs** based on 1-Known reaction sequence and enzymes of the pathway, 2-Significance level, 3-Genes with unknown metabolic function or distal from the pathway. **Sequence of traits** in each row based on GWAS p-value (P) with traits in bold corresponds to lead SNP and provided most significant P; [V] Discovered by looking up the genome-wide mQTLs in the remaining GWASs using P <1E-5. **References** found to be related to components of the kynurenine pathway in previous studies.*

Pathway-specific signals (enzyme mQTLs)

A total of twelve identified signals *(mQTL 4-15, Table 1)* were found within or close to six genes (nearest genes) encoding enzymes known to be involved in catabolism of Trp: IDO1/2, AFMID, KMO, KYNU, HAAO and AADAT. Hits near *IDO1/2, KMO, KYNU* and *AADAT* were associated with several of the measured metabolites (*Fig. 2A&C*); whereas the two mQTLs in the *AFMID* gene (encoding the enzyme producing Kyn from fKyn) affected AA only. For the traits KA, HAA and XA, significant signals were detected near one or several of the immediate upstream or downstream enzyme genes (*Fig. 2C*). A shared genetic determinant for Kyn and the downstream neurotoxic QA was found at *IDO1/2* (*mQTL 4),* responsible for the first immune modulated step of the pathway in extrahepatic tissue. Interestingly, the *mQTL 22 (ATXN2/SH2B3)* also affected both Kyn and QA in a similar fashion, demonstrating the close metabolic link between these kynurenines in the context of immune activation. This may also underpin their strong correlation in plasma (*r2=0.67, Fig. S3*). The overall strongest association for a single metabolite was found at the *AFMID mQTL 5* associated with AA *(rs112281307, P = 1.09E-41).*

Transport system signals (transporter mQTLs)

Four signals (*mQTLs 1-3* and *17)* are located within or near transporter genes with both previously established and unknown relationships to the pathway (*Table 1*). The *mQTLs 1-3,* associated with Kyn and Kyn/Trp, reside near the gene encoding Solute Carrier Family 7 Member 5 (SLC7A5) which is a subunit of the heterodimer light chain-associated amino acid transporter LAT1-4F2hc (SLC7A5-SLC3A2) (29) responsible for importing branched and aromatic neutral amino acids including L-Trp and Kyn. The XA-associated marker *rs1408273 (mQTL 17)* is located within the intron region of *SLC17A3,* in linkage disequilibrium (LD) with the missense *rs1165196,* encoding the SLC17A1 transporter that is known to mediate urate efflux with high expression in kidney tubular cells and moderate expression in hepatocytes (30).

Other signals

Several of the detected mQTLs (*mQTL 16, 18-21, Table 1*) implicate enzymes that have previously not been directly implicated in the kynurenine pathway but to other vital metabolic reactions: UDP glucuronosyltransferase family 1 member A4 UGT1A4 is involved in phase II transformation and conjugation. Although it is possible that kynurenines can undergo conjugation reactions, including glucuronidation, this has not been demonstrated in human tissues. However, this association is an indication that UGT1A4 may be directly or indirectly

implicated in kynurenine metabolism. Four mQTLs of Pic GWAS including the urea-cycle rate-limiting Carbamoyl phosphate synthase 1 CPS1, the Acyl coenzyme A (coA) synthetase medium-chain family member 2B ACSM2B involved in fatty acid metabolism and the Dipeptidase DPEP1 involved in glutathione (γ-Glutamylcysteinylglycine) degradation (31). The *mQTL 22* (*ATXN2/SH2B3*) encodes LNK/SH2B adapter protein 3, a negative regulator of cytokine/growth factor signaling.

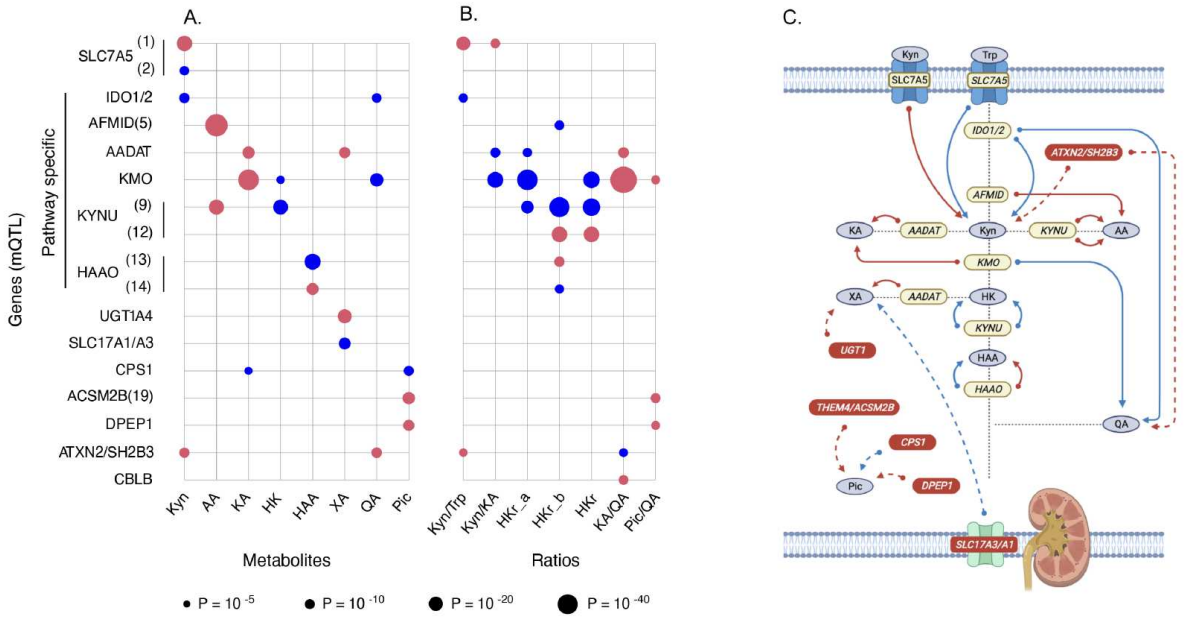


Figure 2.

Genetic determinants and shared loci of metabolites and ratios of the kynurenine pathway

Comparison of effect directions and shared signals across all kynurenines (A) and ratios (B) and Illustration of signals (C). Effect directions in all panels are defined according to the effect of the minor allele (EA).

Colors of dots/arrows indicate if the EA causes a decreasing (blue) or increasing (red) effect.

A and B: *Dot sizes are proportional to −log10(P-val). Metabolite/ratio acronyms shown on x axis. Gene symbols of top hits shown on y axis with numbering of mQTLs shown for loci with multiple hits.*

C: *Illustration of genome-wide signals shown in A (P<5E-08) and THEM4 (P=8.61E-08) that converges with ACSM2B on fatty-acid oxidation. Within-pathway hits are indicated by solid lines and hits with no direct links to the metabolite are indicated by dashed lines and red colors.*

Abbreviations: Trp tryptophan, Kyn kynurenine, AA anthranilic acid, KA kynurenic acid, HK 3-hydroxykynurenine, XA xanthurenic acid, HAA 3-hydroxyanthranilic acid, QA quinolinic acid, Pic picolinic acid, HKr HK/(KA+XA+AA+HAA). HKr_a HK/(KA+XA), HKr_b HK/(AA+HAA), SLC7A5 subunit of the heterodimer light chain-associated amino acid transporter SLC7A5-SLC3A2, AFMID arylformamidase, IDO1/2 indoleamine 2,3-dioxygenase, AADAT kynurenine/alpha-aminoadipate aminotransferase, KYNU kynurenase, KMO kynurenine 3-monooxygenase, HAAO 3-hydroxyanthraniliate 3,4-dioxygenase, SLC17A Solute carrier renal urate transporter, UGT1(A4) UDP glucuronosyltransferase family 1 (member A4), CPS1 Carbamoyl phosphate synthase 1, ACSM2B Acyl-coenzyme A synthetase medium chain family member 2B, THEM4 Acyl-coenzyme A thioesterase, ATXN2 Ataxin-2, SH2B3 LNK/SH2B Adaptor Protein 3.

GWAS on metabolite ratios

We performed GWAS on metabolite ratios including Kyn/Trp, three pathway-balance ratios (Kyn/KA, KA/QA, Pic/QA) and three ratios (HKr, HKr_a, HKr_b) reflecting vitamin B6 status. In addition to recapitulating loci found for individual metabolite GWAS, ratio-based GWAS revealed additional loci in genes responsible for metabolic reactions that have not been found in recent metabolomic-GWAS. HKr, HKr_a and HKr_b, designed to capture the B6-dependent enzymes (AADAT/KYNU), shared several genetic signals with each other *(Fig. 2B)*. Apart from the shared loci with HKr and HKr_a at *KYNU* (*mQTL 9-10, 12)*, HKr_b GWAS found one additional independent *KYNU* signal at *mQTL 11 (Table 1, Table S2).* HKr_b also shares two loci with its component metabolites AA at *AFMID (mQTL5)* and HAA at *HAAO (mQTL13).* The KA/QA GWAS identified an uncharacterized locus near the gene *CBLB* encoding an E3 ubiquitin-protein ligase involved in signal transduction of B/T-cell receptors and high affinity immunoglobulin epsilon receptors (31) with no established mechanistic pathway that is linked to either KA or QA (*Table 1, Fig. 2B)*.

The strongest signal for GWAS on ratios was found for KA/QA-increasing *mQTL7 (P = 1.55E-58),* an intron variant with MAF=0.217 for CEU (dbSNP v157), mapped to KMO, previously known to be related to both kyrurenate and quinolinate levels. In our study, this *mQTL7* is also a hit for both KA *(P = 7.29E-36)* and QA *(P = 1.67E-15) (Fig 2, Table 1)*. Linkage disequilibrium (LD) analysis of the significant variants (*Fig 3A-C.*) reveals three distinct LD blocks whereof the lead SNP, *rs61825638_T,* occupies the third block. As shown in Fig. 3C, this lead SNP is in mild LD with only a few SNPs in the same block ($r^2 < 0.4$).

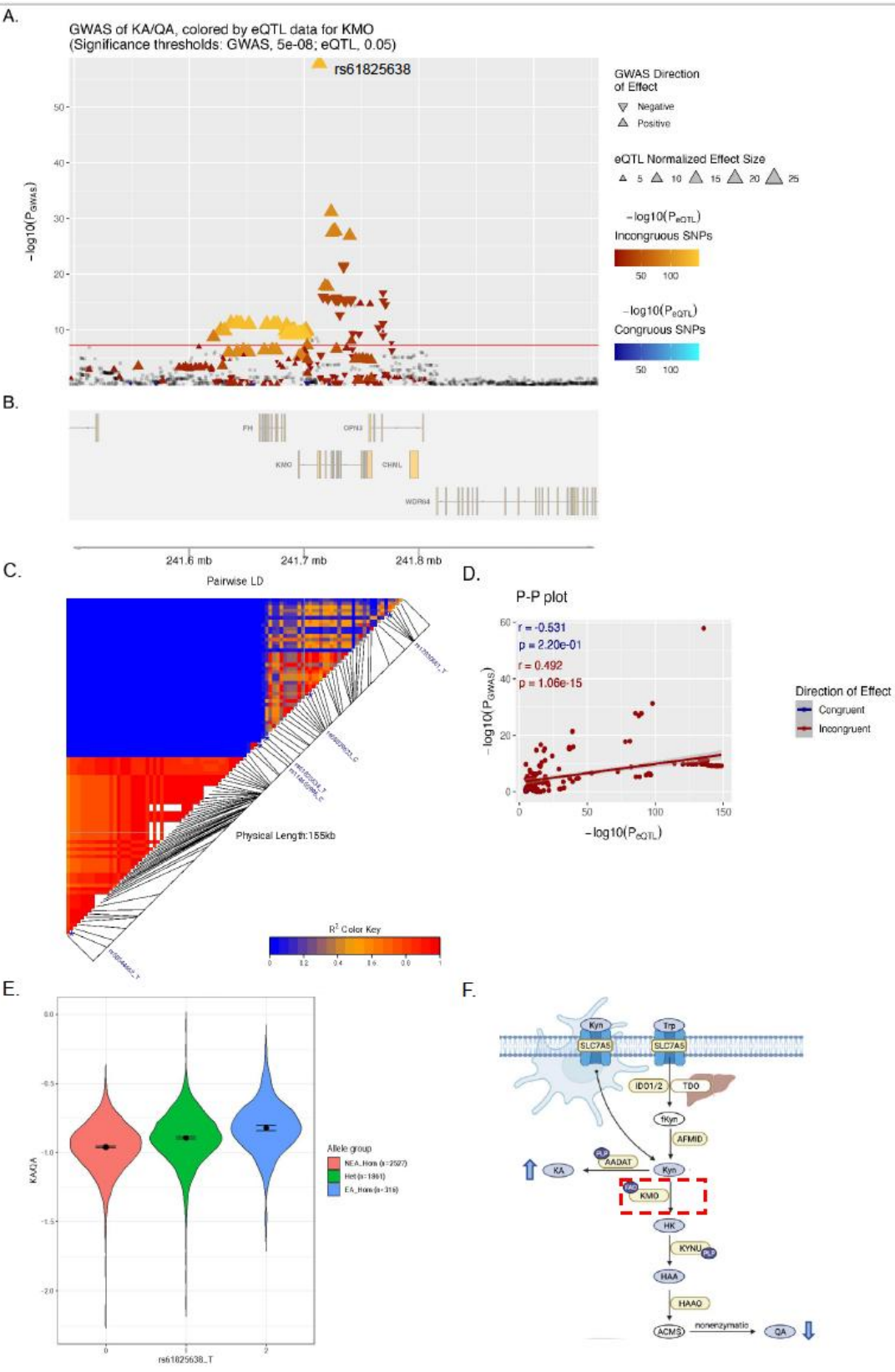


Figure 3. KA/QA GWAS variants colocalize specifically with eQTL SNPs modulating KMO expression in blood and Log(KA/QA) stratified by genotype dosages at rs61825638_T. A. *Co-plotting of KA/QA GWAS signals with KMO eQTL SNPs, with inverse GWAS log(P-val) plotted on the y axis and the red horizontal line indicating GWA P-val = 5E-8. The lead SNP*

rs61825638 is labeled with GWAS P-val = 1.55E-58 and eQTL P-val = 2.68E-136. Plotted triangles are SNPs with eQTL effects for KMO (P < 0.05), with color gradients corresponding to the significance of eQTL P-vals. The size of each triangle corresponds to the normalized eQTL effect size, and the directionality of each triangle corresponds to the GWAS effect direction: congruent SNPs are associated with the same effect direction for both KMO expression levels and KA/QA ratios, whereas incongruent SNPs have opposite effect directions for KMO levels and KA/QA ratios. B. Depiction of the genomic positions of all genes within the 200-kb flanking region centered by rs61825638. C. Heatmap of pairwise linkage disequilibrium (LD) measurements of the 94 significant GWAS SNPs at the KMO locus. SNPs in blue along the diagonal line are representatives for each LD block. D. Correlation plot of GWAS P-vals and eQTL P-vals showing clear evidence of correlation between eQTL P-vals and GWAS P-vals for incongruous SNPs only (Pearson correlation r = 0.492, P = 1.06E-15). E. Log(KA/QA) across individuals carrying different numbers of rs61825638_T. Error bars are shown as mean and 95% confidence interval (95% CI). The number of individuals homozygous for the effect/non-effect allele (EA_Hom/NEA_Hom) or heterozygous (Het) are shown. The 95% CI values from left to right are: NEA_Hom = (-0.967, -0.953); Het = (-0.904, -0.887); EA_Hom = (-0.843, -0.802). F. The two branches of the kynurenine pathway that produce KA and QA, in which KMO plays a critical branching-point influencing KA/QA level. Arrows illustrate the effect directions of rs61825638_T on KA and QA.Abbreviations: KA/QA, kynurenic acid/quinolinic acid ratio; KMO, kynurenine 3-monooxygenase; eQTL, expression quantitative loci. Panels A, B and D were generated by eQTplot, panel C by LDlinkR, panel E by ggplot2 and panel F was modified from Fig. 1.

We investigated whether SNPs found by our GWAS could modulate expression levels of nearby genes (cis-eQTL) in blood by integrating our data (94 SNPs) with summary statistics from the eQTLGen consortium (33). As shown in *Fig. 3A-D,* our GWAS variants (increasing KA/QA) colocalize specifically with eQTL SNPs associated with opposite effects (incongruous, color-coded yellow), in other words decreasing expression levels of KMO in blood (P-P Pearson correlation r =0.492, *P = 1.06E-15*) including the lead SNP *rs61825638 (eQTLGen -P = 2.68E-136)* (*Table S4*). Comparison of Log(KA/QA) stratified by genotype dosages in HUSK demonstrates additive genetic effect pattern of *rs61825638,* as shown in *Figure 3E*.

Molecular annotation of the identified mQTLs

Four of the thirty-one lead SNPs encode amino acid changes of which *rs72897843* (*AFMID,* p.Arg151Trp) is the only coding variant predicted to have a possibly damaging effect on protein function (by Variant Effect Prediction/PolyPhen). Further putative coding and splice variants were found in high LD (r2>=0.8) with lead non-coding SNPs at *ATXN2, ACSM2B* and *SLC17A3* (*Table S3*). Two thirds of all lead SNPs (23/31) have cis-eQTL effects in blood (*Table S4*) and six lead SNPs are also protein-QTLs (pQTLs) or in LD with a pQTL-SNP (*Table S5*). Five out of seven missense SNPs are also *cis*- eQTLs of which the shared lead SNP of Kyn, QA, Kyn/Trp and KA/QA *rs653178 (ATXN2/SH2B3)* has both eQTL and pQTL effect (*Tables S4&5, Fig 2*).

Cross-phenotype analysis

We interrogated the identified mQTLs using Phenoscanner(34) and SNiPA(35) databases for previously published trait-GWAS. The annotation for Kyn, AA, QA and Pic as well as several ratios' hits revealed associations with common traits such as Body Mass Index

(BMI), pulse rate, blood cell traits and cardiovascular disorders (CVD) including *rs8050771 (SLC7A5), rs653178 (ATXN2/SH2B3), rs6741488 (KYNU) and rs12920969 (DPEP1) (Table 2, Table S7)*. Other biomarker/disease-related hits included *rs887829(UGT1A4)* with phosphate, cholesterol levels and liver or biliary/pancreas problem; *rs113104740*(*AADAT*) with thyroid hormone and *rs76156404*(*AADAT*) with sex hormone binding globulin (SHBG) (*Table 2, Table S6)*. The missense *rs72897843(AFMID)*, influencing AA and HKr_b levels, was previously associated with levels of glycated hemoglobin in the UK Biobank (UKBB). The missense *rs3816182(HAAO),* a mQTL of HAA and HKr_b*,* possesses known association with estrone 3-sulfate (*Table S6*) and several clinical conditions such as mesothelioma, ascites, bronchiectasis and pleural effusion, as well as with depression in UKBB (*Table S7*).

Table 2: Known associated traits of the identified lead SNPs

Lead SNP	Nearest gene	HUSK	Known traits *
rs8050771, rs9926829	*SLC7A5*	Kyn, Kyn/KA, Kyn/Trp	Mean corpuscular volume, Mean corpuscular Hb, Pulse rate
rs72897843	*AFMID*	AA, HKr_b	Glycated Hb
rs6741488	*KYNU*	AA	Platelet distribution width, Leukocyte count, Bronchitis, Allergy
rs76156404, rs113104740	*AADAT*	KA, XA, KA/QA, Kyn/KA, HKr_a	Sex hormone-binding globulin, Thyroid hormone levels
rs3816182	*HAAO*	HAA, HKr_b	Mesothelioma, Ascites, Bronchiectasis, Antidepressant treatment
rs887829	*UGT1A4*	XA	Cholesterol, Bilirubin, Liver/Pancreas problem, Cholelithiasis
rs1408273	*SLC17A3/A1*	XA	Urate, IGF1, Mean corpuscular Hb, Glycated Hb, Mineral metabolism
rs1047891	*CPS1*	Pic, KA	eGFR, Blood cell traits, BMI, Chronic Kidney Disease, Cardiovascular traits
rs12920969	*DPEP1*	Pic, Pic/QA	Calcium, Phosphate, eGFR, Hematocrit, Corpuscular volume, Hypertension
rs653178	*ATXN2/SH2B3*	Kyn, QA, KA/QA, Kyn/Trp	HbA1c, Blood cell traits, Urate, Cholesterol, BMI, Allergy, Cardiovascular traits

** Known traits found by cross-phenotype analysis using a cutoff of P<1E-5*
BMI Body Mass Index, eGFR estimated glomerular filtration rate, Hb Hemoglobin, HbA1c hemoglobin A1c, IGF1 Insulin Like Growth Factor 1
HUSK The Hordaland Health Study

Discussion

By performing GWAS on 16 metabolic traits (nine metabolites and seven ratios) measured using a highly precise targeted assay in a population-based sample, we identified 23 mQTLs of which 12 independent loci reside within or in the vicinity of all established pathway-specific genes including *IDO1/2, AFMID, KMO, KYNU, ADAAT* and *HAAO.* Conversely, the same canonical genes affected all eight interrogated kynurenines.

Most major loci identified in the present study replicate findings from previous metabolite GWAS, including signals at SLC7A5, IDO1/2, KMO, KYNU, AFMID, DPEP1 and CPS1 reported in Shin et al., Long et al., Lotta et al., Yin et al. and Surendran et al. The consistency across studies supports the robustness of these loci as central regulators of circulating kynurenine metabolites. Beyond replication, the present study provides the most pathway-complete GWAS of circulating kynurenine metabolites performed in a single cohort with a highly precise targeted assay. This allowed us to extend previous observations by providing simultaneous coverage of a larger set of kynurenine pathway intermediates and biologically informed metabolite ratios, allowing characterization of pathway-wide genetic architecture and identification of additional candidate loci.

Notably, the strongest GWA-metabolite signal overall (at *AFMID*) influenced the peripheral side-branch product AA rather than its core-pathway substrate Kyn. Little is known regarding potential interaction of AFMID and AA in humans; however, AA was previously shown to be an acyl acceptor of kynurenine formamidase in guinea pigs (36).

GWA on the 7 metabolite ratios selected for this study generated hits for the same genes. Many strong hits were found near *KMO* and *KYNU* including the strongest GWA-signal overall found for KA/QA at *KMO*. Several hits in *SLC7A5* confirmed earlier findings of an involvement of this membrane transporter in the metabolism of Trp (25). We also found evidence of important metabolic crosstalk for several genes not directly involved in the pathway. Finally, the data provided tantalizing evidence of a coordinated regulation of Kyn and QA as hits in *IDO1/2* as well as *ATXN2/SH2B* affected both Kyn and QA to the same extent and direction.

To our knowledge, this is the first study to demonstrate that all enzymes in the initial part of the kynurenine pathway, as depicted in *Figs 1/2* may affect the balance of KP intermediates. It is worth mentioning that the relative proportions of each KP intermediates are influenced by different conditions such as inflammatory or hormonal stimulation and dependent on the cellular context. Our plasma mQTLs, assumed to reflect both local and secreted Trp-catabolites, pinpoint an important role for IDO as the first rate-limiting enzyme. It is known that TDO2 controls central metabolism in the liver while IDO is more widely expressed across tissues (16, 17). Notably, tissues such as leucocytes, producing QA in large amounts, utilizes this branch for IDO-mediated immune regulation and NAD^+ synthesis (17). In the context of cancer metabolism, tumour cells utilize KP in order to create immuno-permissive conditions for tumor growth (21, 67), generating various clinical trials targeting IDO1 for cancer treatment. However, the failure of single-target inhibitors in phase III trials has led to the dual inhibition approach (TDO2 and IDO1) (68). The early belief in single-inhibitors may have been influenced by the long-standing concept of the "rate-limiting" IDO1. This concept is challenged by kinetic model analysis which proves that control of KP flux is distributed between several KP enzymes (69). Stavrum et al also concluded that the enzymes tryptophan hydroxylase (TPH) and KMO were major control points in liver and brain along with IDO1 and TDO2 depending on tissue. Other modes of distributed pathway control include interorgan exchange of pathway intermediates and competition of Trp and Kyn for membrane transport in susceptible cell types, with the latter also being dependent on tissue-specific expression of membrane transporters (21). Even though our GWAS study could not stratify flux control implication, the found association strength of IDO1 is overshadowed by several other hits, notably, the strongest KMO, critical for the NAD^+ synthesis branch via QA.

This has direct implications for the outlook and design of effective cancer treatment, but may also apply to therapies targeting neuropsychiatric disorders.

Due to their opposing effects on the NMDA receptor, the balance of KA to QA is considered of prime interest in neurology (21). Conceptually, this would be expected to depend on the activity of KMO. In line with such expectations, the ratio KA/QA captured a remarkably strong signal near KMO, indeed strongest for all the studied ratios. We also found support for a role for ADAAT in this balance, but with a considerably weaker signal. The *mQTL 7(KMO)* which also affected levels of HK and the ratio Pic/QA in this study demonstrate a critical branching role for KMO. The locus has previously shown an association with depression treatment by Prothiaden in the UKBB cohort *(P = 3.56E-04).* Furthermore, integrating our results with eQTLGen data shows that the KA/QA-increasing *rs61825638_T* allele is specifically associated with lower expression of KMO in blood. This suggests that there is a clear dose-dependent effect of KMO on the entire pathway balance and we show that *rs61825638_T* is strongly associated with an increase in the KA-producing branch, concomitant with a decrease in the core-backbone pathway flux. Another notable finding is that KA/QA was associated with a previously unrecognized signal at *CBLB (mQTL 23*) which encodes an E3 ligase involved in protein-ubiquitination and also a vital T-cell gatekeeper (56). The role of CBLB in maintaining immune homeostasis seems to be in line with the known effector function of Trp catabolism operated through the AHR axis. Strikingly, KA/QA levels were also influenced by SH2B3 (*P = 1.12E-07*), the key cytokine-signaling regulator with known interactions with CBL E3 ligase (32). These findings expand the connections between Trp catabolism and immune regulation and suggest unexplored regulators that might be involved in this complex metabolism-immune crosstalk.

Additionally, a previous HUSK study showed that the activity of KMO is conditionally dependent on riboflavin (a precursor of FAD) status, in particular at low PLP (B6) level (70). We also included ratios that have previously been proposed as functional markers of vitamin B6 (PLP) status. Our GWAS findings are in agreement with this concept as SNPs in ADAAT and KYNU affected the ratios in a predictable manner, however, the results also demonstrate further complexity as signals were also picked up in the adjacent KMO and HAAO. Better vitamin B6 status shifts the balance towards less neurotoxic HK and more KA and XA. Thus, vitamin B6 supplementation could provide an easy way of influencing some KP-intermediates in difficult to access compartments such as brain/neurons. Overall, these results indicate that any attempt to control the KP in therapeutic settings should take vitamin B6 (and possibly B2) status into account with HKr offering a direct way to monitor status and progress.

We also discovered mQTLs that have not previously been linked to levels of downstream metabolites of the kynurenine pathway. Pic was associated with variants at distant enzymes (DPEP1, ACSM2B, CPS1) rather than any of the known pathway enzymes. The *rs12920969 (DPEP1)* was associated with homocysteine levels in a meta-analysis of 4,4147 Europeans (38) and is related to a wide range of clinical traits. DPEP1 is a kidney-membrane dipeptidase that participates in the glutathione pathway (31), a process shown previously to be related to the core-pathway HAA (39). A recent genetic analysis on the acyl-CoA medium-chain ligases (ACSMs) addressed that there is a knowledge gap for *ACSMs* genetic variation despite their important roles in fatty acid and xenobiotics metabolism (40). The liver ACSM2 enzyme is known to convert medium-chain fatty acids to the activated acyl-coA

forms for mitochondrial beta-oxidation and also foreign compounds such as benzoate and salicylate for glycine-mediated detoxification (40). We identified *ACSM2B (mQTL19),* a missense variant that was previously linked to phenylacetate (26), pulse rate and viral meningitis (*P=7.98E-04* and *P=9.79E-05*) in UKBB (34). Interestingly, our Pic GWAS also detected a signal at *THEM4 rs28415528* (*P=8.61E-08*) encoding a thioesterase involved in hydrolysis of acyl-CoA compounds including fatty acids (41), supporting the link between Pic and lipid metabolism as shown by ACSM2B. The *rs2841552* was previously associated with nonanoyl carnitine (26), an esterified medium-chain acyl-carnitine among the useful markers of lipid-related traits (42). In addition, recent studies have shown a positive association between fatty-acid oxidation and Trp catabolism in carnitine-depleted rats (43) and suggested a potential link between Pic and microvascular protection in type 1 diabetes (44). Lastly, the association of *rs1047891(CPS1)* with Pic might be attributed to pleiotropic effects/high connectivity of metabolic networks as shown in previous GWAS; however, it may also relate directly to the known involvement of Pic in L-arginine-metabolism (45). Another notable finding is the XA-associated 2q37.1 locus (*mQTL 16*), encoding UDP glucuronosyltransferase family 1 member A4 (UGT1A4) involved in phase II transformation, conjugation and efflux of lipophilic molecules. This locus is part of the *UGT1A* gene cluster composed of 13 exons whereof SNPs have been associated with circulating metabolites such as thyroxine, heme-bilirubin/biliverdin and many bilirubin-oxidized compounds (26). Xanthurenate-8-O-β-D-glucoside has been detected in human urine (42), thus, UGT1A4 could be the key UDP-glucosyltransferase in downstream reactions that utilize XA. The XA-associated SLC17A3 (*mQTL17*), is a voltage driven transporter located on the renal proximal tubule ‘s apical side, known to transport a wide variety of organic anions such as estrone sulfate and estradiol-17-β-glucuronide (31). This locus was previously shown to be associated with urate levels (47), mineral metabolism, hemoglobin concentration, mean corpuscular volume as well as pathological conditions such as primary sclerosing cholangitis (48), rheumatoid arthritis (49) and coeliac disease (35). Why the *SLC17A3* and *UGT1A4* associations seem restricted to only XA among the kynurenines are not clear; however, previous studies in rats have shown that XA is transported by the renal proximal tubule transporters and XA infusion can indeed stimulate diuresis in rats (50, 71).

We also expanded the genetic catalogue of Trp metabolism to *SNP - metabolic marker – disease links*. The ratio Kyn/Trp (KTR) has been studied extensively with respect to IDO1 activation and inflammaging conditions (2, 11, 19). The association of both *ATXN2/SH2B3* and *IDO1/2* with not only Kyn or QA but also for the inflammatory-marker Kyn/Trp could indicate a link to the upregulation of IDO1 via immune activation. Besides catalyzing the conversion of Trp towards Kyn, IDO1 is known to have immunoregulatory as well as signal transduction function (18, 46). The noncatalytic domain of IDO1 can be tyrosine-phosphorylated and thus promote activation of the noncanonical nuclear factor-κB (NF-κB) pathway, which in turn self-enhances IDO1 transcription. Interestingly, *rs653178,* the lead SNP of *mQTL22,* is in almost complete LD with *rs3184504* encoding a well-known missense variant at *SH2B3* (32). LNK/SH2B3 is involved in hematopoiesis, cytokine-signaling and was previously associated with a wide range of traits and diseases. A recent *in vivo* study has identified differential Kyn levels in blood, brain and adipose tissues between SH2B3-knocked out and wild-type mice (51). In addition, several known pQTLs of the *ATXN2/SH2B3* hit are indeed immune-modulators such as the IL-2 receptor subunit alpha. Thus, we postulate that the effectors of *mQTL22* might be involved in the fine-tuning of IDO1-mediated signaling, via a yet to be fully characterized genetic-metabolic control.

Our study has both strengths and limitations. Strengths of the present study include the use of a targeted metabolomic method that covers most components of the kynurenine pathway, including several low-abundance metabolites that previously have been implicated in a variety of common diseases. The method includes an isotope-labelled internal standard for all Trp-catabolites, which provides high analytical precision and accuracy (57). Such analytical performance may partly explain the large number of GWA signals detected for the comparatively small number of metabolites included in the study. The analysis included only common variants genotyped from individuals of northern European ethnicity. While this ensures a homogenous and well-powered design, it may limit generalizability of the results to other populations. Another potential limitation is that samples were non-fasted/collected without information about fasting-status.

In conclusion, by using a targeted metabolomic assay, we were able to characterize the genetic influences on the Tryptophan catabolism pathway at comprehensive pathway-level resolution. The traits include isolated metabolites and metabolite ratios previously studied in relation to disease risk including inflammaging, neuromodulation and vitamin B6 status. We identified 23 independent mQTLs pinpointing known loci within or near genes encoding enzymes with an established role in the pathway and previously uncharacterized loci associated with pathway regulation as well as with immune homeostasis. Furthermore, we discovered loci linked to distal processes including fatty acids oxidation, urate transportation and phase II transformation/efflux processes. These observations should motivate further investigations of possible crosstalk between the kynurenines pathway and other biological processes and may provide instruments for future studies on the role of the kynurenine pathway in the pathogenesis of common diseases using causal inference approaches.

Materials and Methods

Study population, clinical measures and biochemical platform

HUSK is a population-based health survey performed in the Hordaland County of Western Norway (https://husk-en.w.uib.no/). The study was approved by the Regional Committee for Medical and Health Research Ethics, REK West, Norway (REK West #2015/1763) with informed consent from all participants (28) and performed in accordance with the Declaration of Helsinki. The participants were born during 1925-1927 (*N*=3,341) or 1950-1951 (*N*=3,733)(28). Baseline data collection during 1997-1999 included self-reported lifestyle and health behavior questionnaires, measurements of height, weight, waist and hip circumference. Smoking status as binary (yes/no) was also self-reported. Systolic and diastolic blood pressures were reported as the mean of three consecutive measurements. Plasma lipids and glucose levels were measured at Ullevål University Hospital, Oslo, Norway.

Baseline, non-fasting plasma concentrations of Trp, Kyn, KA, AA, HK, HAA, XA, QA, Pic were measured by targeted liquid chromatography-tandem mass spectrometry (LC-MS/-MS) (58) at Bevital AS, Bergen, Norway (www.bevital.no). The precision for the targeted LC-MS/-MS assay ranged from 3-8 % for within-day coefficient of variation (CV), and 4-10% for between-day CV. The limit of detection for the assay ranged from 0.4 nmol/L to 0.12 µmol/L.

Genotyping, quality control, relatedness and population structure

Genotyping was available for 6,707 samples genotyped using the Illumina HumanCoreExome-12 v.1.1 (542,585 markers) at the Norwegian University of Science and Technology, Trondheim, Norway. The Genome Reference Consortium Human Build 37 (GRCh37) was used for annotating all genotyped autosomal polymorphisms (SNPs). We performed genotype quality control (QC) using PLINK 1.9(59) with the following criteria a) sample call rate >=98%, b) marker call rate >=98%, c) heterozygosity rate <=4SD, d) minor allele frequency (MAF)>=1%, e) deviation from Hardy-Weinberg equilibrium (HWE) <1E-6, f) sex check (X chromosome homozygosity [Female <0,2 and Male >0,8]).
By comparing our data with the Northern and Western European ancestry residents in Utah, USA (CEU) and other populations of the HapMap v3 project(60), we filtered out non-CEU or admixture samples and obtained a core-sample set of 4,931 individuals for association analysis. Details of QC are shown in the supplementary information.

Variant imputation

The reference panel was downloaded from the Haplotype Reference Consortium (HRC) version 1.1(61).
Compatibilit**y** between our data and HRC panel including marker name and position, strand orientation, strand ambiguity, allele matching was checked using the imputation preparation tool by Will Rayner version 4.2.5(62). A total of 367258 markers remained eligible for pre-phasing and imputation. Pre-phasing and imputation were performed via uploading to the Sanger imputation server with SHAPEIT2 and positional Burrows-Wheeler transform pipeline. After that, SNPs with INFO score (INFO) lower than 0.7 were filtered out.

Metabolite processing

We included 16 metabolomic traits in the primary GWAS-analysis: Nine metabolites including Trp, the kynurenines, as well as seven biomarker-derived ratios described in *Table S1B.* All metabolites or metabolite-ratios were log-transformed. Histograms of each metabolite/ratio were plotted and Spearman coefficients for each pair of metabolites were computed using the PerformanceAnalytics package in R.

Statistical analysis for genetic associations

We investigated the association between each metabolite/ratio with imputed hard celled genotypes (MAF>=1%, INFO>=0.7) using the linear regression function of PLINK v1.9 under the assumption of an additive genetic model and with age, gender, BMI, creatinine and smoking as covariates. BMI was adjusted based on previous observation(63). A sensitivity analysis was performed on the same metabolites without adjustment for creatinine (as a proxy of renal function) which revealed equivalent results (data not shown).
Significant associations were assigned to each metabolite or ratio by selecting SNPs passing the Bonferroni-corrected GWA threshold (P < 5E−8). The most significant SNP of each 1Mb-clumped region was considered as the lead SNP per region (mQTL). Independent mQTLs were discovered by stepwise-conditional regression on the lead SNP using PLINK v1.9. We created Manhattan and Q-Q plots using our in-house code (https://github.com/chinhbn/qqman) adapted

from the qqman package (64). Regional plots illustrating the 500kb-flanking region of the index SNP were generated using LocusZoom v1.3.

Annotation of genetic signals

Locus naming: Each locus was named according to the gene in closest vicinity to the lead/index SNP (within 100kb). We used the PhenoScanner v2 R command tool to query the University of Cambridge's PhenoScanner database (34) for molecular annotation of the lead SNPs using the 1000 Genomes phase 3 (1000G p3) v5(65) per September 2021. We used a LD threshold of r2>=0.8 to expand index SNPs to correlated SNPs in the PhenoScanner database and collected the following information (*P* <1E-5): variant consequences; protein quantitative trait (pQTL); known associated metabolites and clinical traits. Local gene expression quantitative trait (*cis*-eQTL) in blood was annotated using the eQTLGen database. We looked for previously reported eQTL using a False Discovery Rate (FDR) < 0.05, pQTL and known associated traits using *P* <1E-5, mQTLs in the SNiPA v3.3 database (35) using *P* <1E-4.

Detection of shared mQTLs across the metabolites and ratios

For each identified index SNPs, we compared the results across all tested metabolites and ratios in the study. We used a threshold of *P* <1E-05 for any additional trait, to define an mQTL as shared across metabolites/ratios.

eQTL colocalization analysis

Statistical analysis and visualization of the colocalization between KA/QA GWAS hits and blood *cis*-eQTLs at chromosome 1 were done using the eQTpLot package, available at https://github.com/RitchieLab/eQTpLot. LD heatmap between pairs of SNPs was generated using GRCh37 physical genetic distance by the LDlinkR package (https://github.com/CBIIT/LDlinkR)

Enrichment of gene-level signals using GTEx tissue-specific gene expression

Enrichment results of differentially expressed genes (up/down-regulation) into tissue-specific patterns were obtained using FUMA v1.3.6a(66) encompassing the 1000G p3, MAGMA v1.09 algorithm with the use of log2-transformed transcript per million from version 7 of the tissue-specific gene expression database GTEx.

Digital secure server

All genotype QC, association analyses and post-GWAS processing were performed using digital secure labs in the HUNT Cloud provided by the Norwegian University of Science and Technology, Trondheim, Norway.

Data availability

In accordance with the General Data Protection Regulation (GDPR, https://gdpr-info.eu/), individual-level clinical, genetic and proteomics data in the HUSK study cannot be made publicly available to maintain participant confidentiality, but can be made available to researchers, provided approval from the Regional Committees for Medical and Health Research Ethics (REC), compliance with the EU General Data Protection Regulation

(GDPR) and approval from the HUSK study (_https://husk-en.w.uib.no/). Complete summary statistics from the GWAS of metabolites and ratios in the current study are available in Zenodo (http://doi.org/10.5281/zenodo.23613886).

Acknowledgments
This work was supported by grants (to Stefan Johansson) from Helse Vest's Open Research (no. 912250 and F-12144), the Novo Nordisk Foundation (NNF19OC0057445) and the Research Council of Norway (no. 315599)) and (to Pål Rasmus Njølstad) from the European Research Council (AdG SELECTionPREDISPOSED no. 293574), the Bergen Research Foundation (Utilizing the Mother and Child Cohort and the Medical Birth Registry for Better Health), the University of Bergen, the Research Council of Norway (FRIPRO no. 240413), the Western Norway Regional Health Authority (Strategic Fund Personalized Medicine for Children and Adults), and the Novo Nordisk Foundation (no. 54741). This work also received support from the Research Council of Norway (Better Health by Harvesting Biobanks (no. 229624)). The authors thank Marc Vaudel, Haydee Maribel Artaza Alvarez and Kari Juul at University of Bergen, Oddgeir Lingaas Holmen at Norwegian University of Science and Technology.

Reference list
1. Badawy, A. A. B. Kynurenine pathway of tryptophan metabolism: Regulatory and functional aspects. Int. J. Tryptophan Res. 10 (2017). https://doi.org/10.1177/1178646917691938
2. Sulo, G. et al. Neopterin and kynurenine–tryptophan ratio as predictors of coronary events in older adults. Int. J. Cardiol. 168, 1435–1440 (2013). https://doi.org/10.1016/j.ijcard.2012.12.073
3. Cole, J. E. et al. Indoleamine 2,3-dioxygenase-1 is protective in atherosclerosis. Proc. Natl Acad. Sci. USA 112, 13033–13038 (2015). https://doi.org/10.1073/pnas.1517820112
4. Huang, Y. S. et al. IDO and kynurenine metabolites in peripheral and CNS disorders. Front. Immunol. 11 (2020). https://doi.org/10.3389/fimmu.2020.00388
5. Dagenais-Lussier, X. et al. Latest developments in tryptophan metabolism. Cytokine Growth Factor Rev. 59 (2021). https://doi.org/10.1016/j.cytogfr.2021.01.003
6. Zuo, H. et al. Interferon-γ-induced inflammatory markers and the risk of cancer. Cancer 120, 3370–3377 (2014). https://doi.org/10.1002/cncr.28832
7. Cervenka, I., Agudelo, L. Z. & Ruas, J. L. Kynurenines: Tryptophan's metabolites. Science 357 (2017). https://doi.org/10.1126/science.aaf9794
8. Keaton, S. A. et al. Altered tryptophan catabolism in placentas from women with preeclampsia. Int. J. Tryptophan Res. 12 (2019). https://doi.org/10.1177/1178646919840321
9. Hafstad Solvang, S. E. et al. Kynurenines and cognitive prognosis. Int. J. Tryptophan Res. 12 (2019). https://doi.org/10.1177/1178646919875134
10. Campbell, B. M. et al. Kynurenines in CNS disease. Front. Neurosci. (2014). https://doi.org/10.3389/fnins.2014.00012
11. Sorgdrager, F. J. H. et al. Tryptophan metabolism in inflammaging. Front. Immunol. 10 (2019). https://doi.org/10.3389/fimmu.2019.02569

12. Ostapiuk, A. & Urbanska, E. M. Kynurenic acid in neurodegeneration. CNS Neurosci. Ther. 28, 19–35 (2022). https://doi.org/10.1111/cns.13784
13. Morrens, M. et al. Kynurenine pathway alterations in schizophrenia. Schizophr. Res. 223, 43–52 (2020). https://doi.org/10.1016/j.schres.2020.07.015
14. Brundin, L. et al. Kynurenine pathway enzyme and suicidal behaviour. Transl. Psychiatry 6 (2016). https://doi.org/10.1038/tp.2016.178
15. Savitz, J. The kynurenine pathway. Mol. Psychiatry 25, 131–147 (2019). https://doi.org/10.1038/s41380-019-0414-4
16. van der Goot, A. T. & Nollen, E. A. A. Tryptophan metabolism and aging. Trends Mol. Med. 19, 336–344 (2013). https://doi.org/10.1016/j.molmed.2013.02.001
17. Moffett, J. R. et al. Quinolinate as marker. Front. Immunol. 11, 31 (2020). https://doi.org/10.3389/fimmu.2020.00031
18. Orabona, C. et al. SOCS3 drives degradation of IDO. Proc. Natl Acad. Sci. USA 105, 20828–20833 (2008). https://doi.org/10.1073/pnas.0810278105
19. Deac, O. M. et al. Immune biomarkers and tryptophan metabolism. J. Nutr. 146, 1801–1806 (2016). https://doi.org/10.3945/jn.116.234146
20. Ulvik, A. et al. Tryptophan catabolites and vitamin B6 status. Am. J. Clin. Nutr. 111, 178–186 (2020). https://doi.org/10.1093/ajcn/nqz257
21. Platten, M. et al. Tryptophan metabolism as therapeutic target. Nat. Rev. Drug Discov. 18 (2019). https://doi.org/10.1038/s41573-019-0016-5
22. Boros, F. A. et al. Genetic alterations of kynurenine pathway genes. Mutat. Res. (2018).
23. Suhre, K. et al. GWAS of metabolic traits. Nat. Genet. 43, 565–569 (2011). https://doi.org/10.1038/ng.837
24. Schlosser, P. et al. Urinary metabolite genetics. Nat. Genet. 52, 167–176 (2020). https://doi.org/10.1038/s41588-019-0567-1
25. Shin, S. Y. et al. Atlas of genetic influences on metabolites. Nat. Genet. 46, 543–550 (2014). https://doi.org/10.1038/ng.2982
26. Long, T. et al. WGS of metabolites. Nat. Genet. 49, 568–578 (2017). https://doi.org/10.1038/ng.3809
27. Lotta, L. A. et al. Genetic regulators of metabolism. Nat. Genet. 53, 54–64 (2021). https://doi.org/10.1038/s41588-020-00767-z
28. Refsum, H. et al. Hordaland Homocysteine Study. J. Nutr. 136 (2006).
29. Verrey, F. System L transporters. Front. Physiol. 445, 529–533 (2003).
30. Uhlén, M. et al. Human proteome map. Science 347 (2015). https://doi.org/10.1126/science.1260419
31. Bateman, A. UniProt database. Nucleic Acids Res. 47, D506–D515 (2019). https://doi.org/10.1093/nar/gky1049
32. Maslah, N. et al. SH2B3 in hematologic disease. Leukemia 31, 1661–1670 (2017).
33. Võsa, U. et al. eQTL analyses. Nat. Genet. 53, 1300–1310 (2021). https://doi.org/10.1038/s41588-021-00913-z
34. Kamat, M. A. et al. PhenoScanner V2. Bioinformatics 35, 4851–4853 (2019). https://doi.org/10.1093/bioinformatics/btz469
35. Arnold, M. et al. SNiPA tool. Bioinformatics (2014).
36. Santti, R. S. & Hopsu-Havu, V. K. Kynurenine formamidase reactions. Acta Chem. Scand. 24, 791–796 (1970).
37. Jones, S. P. et al. Kynurenine pathway expression. PLoS One 10 (2015). https://doi.org/10.1371/journal.pone.0130909
38. van Meurs, J. B. J. et al. Homocysteine genetics. Am. J. Clin. Nutr. 98, 668–676 (2013).

39. Li, S. M. et al. 3-hydroxyanthranilic acid induces T cell death. Immunol. Lett. 132, 53–60 (2010).
40. van der Sluis, R. et al. ACSM2A variation. J. Biol. Chem. 293, 1279–1292 (2018).
41. Hunt, M. C. et al. Peroxisomal lipid metabolism enzymes. Biochim. Biophys. Acta 1822, 1397–1410 (2012).
42. Wishart, D. S. et al. HMDB 4.0. Nucleic Acids Res. 46, D608–D617 (2018). https://doi.org/10.1093/nar/gkx1089
43. Lindquist, C. et al. Kynurenine metabolites and lipid metabolism. Biochim. Biophys. Acta 1865, 158543 (2020).
44. Jain, R. et al. Liver nucleotide biosynthesis and vascular risk. Sci. Rep. 10, 25 (2020). https://doi.org/10.1038/s41598-019-56917-0
45. Melillo, G. et al. Picolinic acid and macrophages. J. Immunol. 150, 4031–4040 (1993).
46. Grohmann, U. et al. Amino-acid sensing in immune regulation. Cytokine Growth Factor Rev. 35, 37–45 (2017).
47. Kolz, M. et al. Uric acid GWAS. PLoS Genet. 5, e1000504 (2009). https://doi.org/10.1371/journal.pgen.1000504
48. Ji, S. G. et al. GWAS PSC. Nat. Genet. 49, 269–273 (2017). https://doi.org/10.1038/ng.3745
49. Okada, Y. et al. Rheumatoid arthritis genetics. Nature 506, 376–381 (2014). https://doi.org/10.1038/nature12873
50. Uwai, Y. et al. Xanthurenic acid effects. Biomed. Res. 35, 223–226 (2014).
51. Bagheri, M. et al. Plasma kynurenine genetics. Sci. Rep. 11, 15652 (2021). https://doi.org/10.1038/s41598-021-95154-9
52. Wirthgen, E. et al. Kynurenic acid Janus-faced role. Front. Immunol. 8, 1957 (2018). https://doi.org/10.3389/fimmu.2017.01957
53. Grant, R. S. et al. Picolinic acid brain action. Int. J. Tryptophan Res. 2, 71–79 (2009). https://doi.org/10.4137/IJTR.S2445
54. Sowa-Kućma, M. et al. KP and white matter bipolar disorder. Eur. Arch. Psychiatry Clin. Neurosci. 268, 157–168 (2018). https://doi.org/10.1007/s00406-017-0801-1
55. Bryleva, E. Y. et al. NMDA receptor modulation depression. Brain Behav. Immun. 43, 110–117 (2015). https://doi.org/10.1016/j.bbi.2014.07.012
56. Lutz-Nicoladoni, C. et al. Cbl-b immune modulation. Front. Oncol. 5, 58 (2015). https://doi.org/10.3389/fonc.2015.00058
57. Ulvik, A. et al. Precision loss metabolomics. Anal. Chem. 93, 7616–7624 (2021). https://doi.org/10.1021/acs.analchem.0c05101
58. Midttun, Ø. et al. LC–MS biomarkers profiling. Rapid Commun. Mass Spectrom. 23, 1371–1379 (2009). https://doi.org/10.1002/rcm.4013
59. Chang, C. C. et al. PLINK second generation. Gigascience 4, 7 (2015). https://doi.org/10.1186/s13742-015-0047-8
60. Belmont, J. W. et al. HapMap Project. Nature 426, 789–796 (2003). https://doi.org/10.1038/nature02168
61. McCarthy, S. et al. Imputation haplotypes. Nat. Genet. 48, 1279–1283 (2016). https://doi.org/10.1038/ng.3643
62. Rayner, W. HRC imputation tools. Available at: https://www.well.ox.ac.uk/~wrayner/tools/
63. Theofylaktopoulou, D. et al. Immune activation determinants. Clin. Exp. Immunol. 173, 121–130 (2013). https://doi.org/10.1111/cei.12092
64. Turner, S. D. qqman R package. J. Open Source Softw. 3, 731 (2018). https://doi.org/10.21105/joss.00731

65. 1000 Genomes Project Consortium. Available at: https://www.internationalgenome.org/
66. Watanabe, K. et al. FUMA mapping. Nat. Commun. 8, 1826 (2017). https://doi.org/10.1038/s41467-017-01261-5
67. Prendergast, G. C., Malachowski, W. J., Mondal, A., Scherle, P. & Muller, A. J. Indoleamine 2,3-dioxygenase and its therapeutic inhibition in cancer. Int. Rev. Cell Mol. Biol. 336, 175–203 (2018). https://doi.org/10.1016/bs.ircmb.2017.07.004
68. Kang, I. et al. Targeting KP cancer immunity. Front. Oncol. 14 (2025). https://doi.org/10.3389/fonc.2024.1524651
69. Stavrum, A. K. et al. Tryptophan metabolism model. J. Biol. Chem. 288, 34555–34566 (2013). https://doi.org/10.1074/jbc.M113.474908
70. Theofylaktopoulou, D. et al. Vitamins B2/B6 KP. Br. J. Nutr. 112, 1065–1072 (2014). https://doi.org/10.1017/S0007114514001858
71. Surendran, P. et al. Genetic determinants metabolism. Nat. Med. 28, 2321–2332 (2022). https://doi.org/10.1038/s41591-022-02046-0
72. Yin, X. et al. GWAS metabolites Finnish men. Nat. Commun. 13, 1644 (2022). https://doi.org/10.1038/s41467-022-29397-5

Supplementary Files

This is a list of supplementary files associated with this preprint. Click to download.

- S.Tabsall.xlsx
- SI.pdf
- SIpage1.pdf